JOURNAL OF MATERIALS SCIENCE 16 (1981) 1097–1102

Studies of a thermomechanically treated Al–Zn–Mg alloy

C. M. WAN, W. Y. WEI, M. T. JAHN
Department of Materials Science and Engineering, National Tsing Hua University, Hsinchu, Taiwan, Republic of China

The influence of subgrain structure on the precipitation process in an Al–4.2 wt % Zn–1.6 wt % Mg alloy was studied and correlated with its mechanical properties for ageing temperatures of 110, 142 and 165° C.

1. Introduction

Much work has been performed in attempts to determine the precipitation sequence of high-strength Al–Zn–Mg alloys. Various precipitation sequences have been proposed to take place during the ageing processes of the alloy system aged below 190° C after being quenched to room temperature [1–5]. In addition, considerable effort has been made to improve the mechanical properties of this alloy system through the presence of substructures produced by certain thermomechanical treatments (TMT). According to Waldman *et al.* [6], Ryum [7] and Holl [8], Al–Zn–Mg alloys can be improved in both strength, ductility and fatigue resistance through various thermomechanical processes.

Since the mechanical properties of materials after such a TMT are the result of the overall and synthetic effects of grain boundaries, subgrain boundaries, dislocations, vacancies, precipitates etc. it is very interesting to study the influence of subgrain structures produced after such a thermomechanical treatment on the precipitation process in aluminum alloys.

According to Ryum [7] and Zakharov [9], almost perfect subgrain structures always accompany the recrystallization process at a very early stage. Holl [8] and Wan *et al.* [10] have studied the influence of subgrain structure on the precipitation-hardening of Al–Zn–Mg alloys aged at 120° C and 165° C, but they found no precipitation inhibiting effect due to the presence of subgrains at lower ageing temperatures.

The influence of plastic strain on the ageing process may usually be of two kinds [11]. First, for the as-quenched material, plastic deformation will remove some vacancies and then retard the formation of Guinier–Preston (G–P) zones in some regions by vacancies sinking to boundaries etc. Second, plastic deformation may provide preferential sites for the nucleation of metastable or equilibrium phases and then accelerate the growth of precipitates.

The work of this study was concentrated in a deeper investigation of the influence and correlations of subgrain structures with the distribution of precipitates and the tensile properties for various ageing temperatures and times. In addition, the serrated yielding, or Portevin–LeChatelier effect, on the as-quenched and briefly artificially aged materials is also studied.

2. Experimental procedure

The chemical composition of the alloy used in this experiment is shown in Table I.

A plate, of thickness 3.1 mm was first annealed at 450° C for 30 min and then rolled to a thickness of 2.46 mm by three passes at high temperature. Two ageing steps were then performed. First, all the specimens were naturally aged at room tem-

TABLE I Chemical Composition of the alloy

Element	Zn	Mg	Mn	Fe	Si	Cu	Ti	Zr	Al
Content (wt %)	4.2	1.55	0.30	0.28	0.14	0.07	0.04	0.13	Balance

0022–2461/81/041097–06$02.60/0

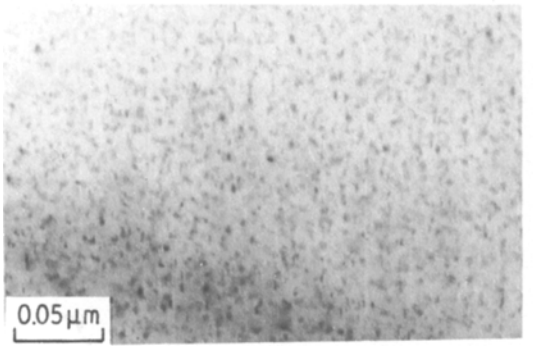

Figure 1 TEM view of specimen aged at 110° C for 24 h.

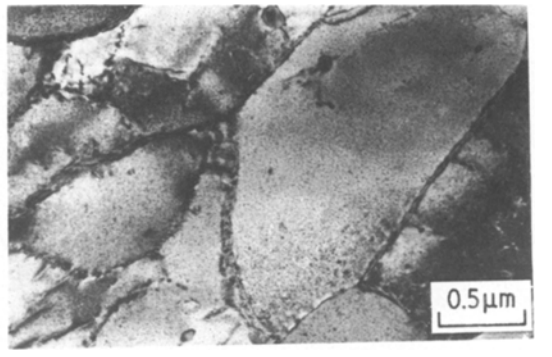

Figure 3 TEM view of specimen aged at 110° C for 192 h.

perature for two months, solution treated at 460° C for one hour, and then quenched in water to room temperature thus forming well-defined subgrains. Second, the specimens were aged at temperatures of 110, 142 or 165° C for various periods of time ranging from 30 min to 16 days. The specimens without subgrains were produced by annealing the as-rolled samples at 550° C for two hours, furnace cooling to 460° C, and were then water quenched.

Tensile tests were performed with an Instron test machine, Model 1115; tensile tests were carried out with cross-head speed of 0.1 cm min^{-1} and 0.2% off-set technique was used to determine the yield strength. Tensile tests performed for the purpose of studying the Portevin–LeChatelier effect were carried out with various cross-head speeds of 0.05, 0.1, 0.5 and 2 cm min^{-1}.

Interior microstructure studies were performed with a JEOL-100B transmission electron-microscope, operating at 100 kV, using the thin foil technique.

3. Results and discussions

According to Polmear [12], the upper temperature limit of stable G–P zones in ternary Al–Zn–Mg alloys is about 128° C. At an early stage of the ageing process, with an ageing temperature of 110° C, we observed fine, densely distributed G–P zones and η'-phase plates of size between 20 and 40 Å in diameter. Some equilibrium η-phase particles were found in the matrix as the samples were aged for longer times, as shown in Figs 1 to 4. η-laths and ledge η-plates were formed mostly on grain boundaries and within some of the subgrains. Fig. 3 shows some small, partial, very narrow, precipitate-free zones on the subgrain boundaries. From the microstructure study performed on the material aged for 16 days, using the technique of selective area diffraction, η-plates on the {1 1 1} planes were observed, as shown in Fig. 4.

Since the temperature of 142° C is higher than the solvus temperature of the G–P zones the apparent density of precipitates in the samples aged at a temperature of 142° C is much less than that for samples aged at a temperature of 110° C. At an early stage of this ageing process, some η-laths nucleated on dislocations and some more-densely distributed η-phase regions were observed

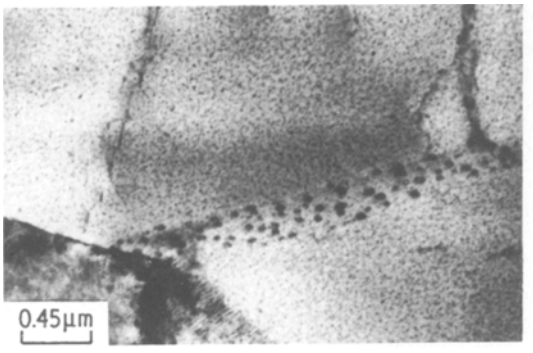

Figure 2 TEM view of specimen aged at 110° C for 120 h.

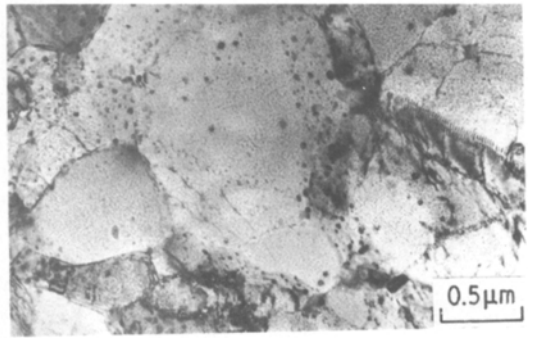

Figure 4 TEM view of specimen aged at 110° C for 384 h.

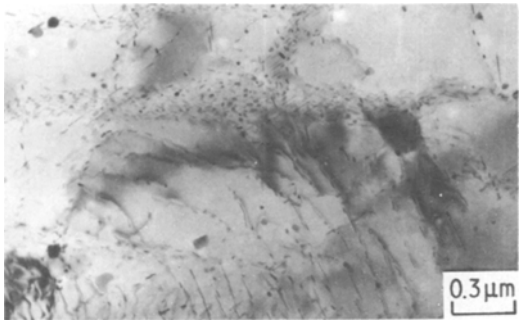

Figure 5 TEM view of specimen aged at 142° C for 6 h.

on the subgrain boundaries, as shown in Fig. 5. The density of η-phase regions increased and their distribution became more uniform inside the subgrains, as the ageing time was increased, as shown in Fig. 6. It was observed that the nucleation of the η-phase is inhibited inside some subgrains; Fig. 7 shows that the η-phase density was high in areas where there were no subgrains.

The microstructures of specimens aged at 165° C for 1, 5 and 40 h are shown in Figs 9, 10 and 11, respectively; the precipitates found in this series are similar to those found in the specimens aged at 142° C.

Most of the equilibrium η-phases found in this work are identified to be η_2, η_4 and η_9 on the classification scheme of Gjønnes and Simensen [3]. The morphology of η_2 was round or hexagonal plates on the {1 1 1} matrix plane. This type was found on the subgrain boundaries using the dark-field transmission electron microscopy technique, as shown in Fig. 4. The other two types of equilibrium η-phase, η_4 and η_9 are similar in morphology. They were all lath-like in shape with the largest dimension parallel to the ⟨1 1 0⟩ matrix direction. The directions of all three phases were determined using the selected area diffraction pattern technique.

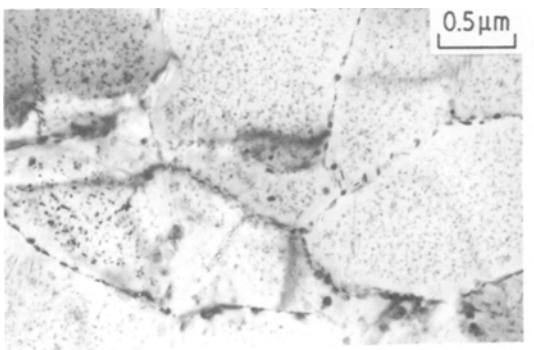

Figure 6 TEM view of specimen aged at 142° C for 16 h.

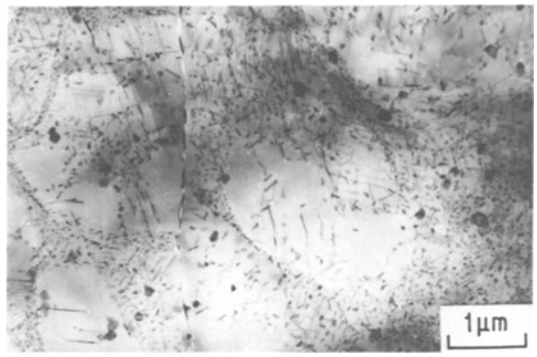

Figure 7 TEM view of specimen aged at 142° C for 64 h.

The η' precipitates are coherent with the matrix on {1 1 1} planes, $d_{10\bar{1}0} = 3d_{220}$, where d is the plane spacing, which is equivalent to the coherent relationship of η-lath, $d_{0002} = 3d_{220}$. This makes it difficult to judge from the diffraction pattern whether the η'-phase is present or not when only one $\vec{g}_{220}$ is operating, where g is the beam direction, especially for the rolled samples where (1 1 0) [1 $\bar{1}$ 2] textures are encountered. Thus, the existence of the η' phase is always judged by the size and shape of those particles which appeared in the samples aged at 110° C.

Consequently, the suggested ageing sequences for the three ageing temperatures are as follows:

$$\text{SSS} \rightarrow \text{G–P zones} \rightarrow \eta' \rightarrow \eta\ (\text{MgZn}_2)$$

(for ageing at 110° C) (1)

and

$$\text{SSS} \rightarrow \eta\ (\text{MgZn}_2)$$

(for ageing at 142° C and 165° C), (2)

where SSS represents saturate solid solution.

With regard to the microstructures in the vicinity of the grain boundaries and subgrain boundaries, according to Unwin *et al.* [13], the width of the grain boundary precipitate-free zone,

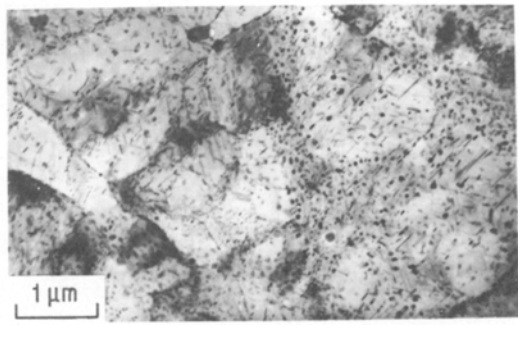

Figure 8 TEM view of specimen aged at 142° C for 64 h.

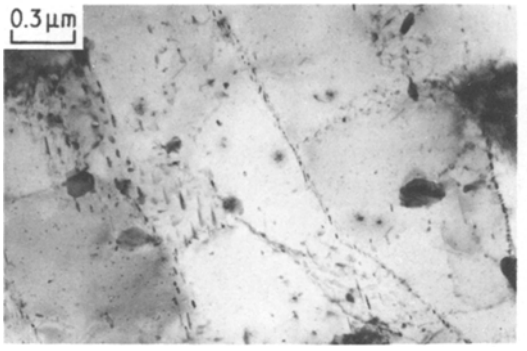

Figure 9 TEM view of specimen aged at 165° C for 1 h.

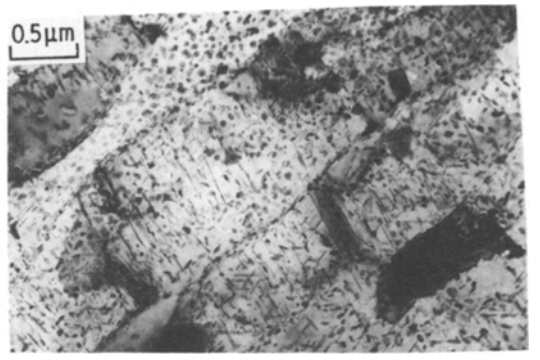

Figure 11 TEM view of specimen aged at 165° C for 40 h.

as well as the nucleation and growth rates of precipitates near the grain boundaries, is controlled mostly by both the vacancy concentration and degree of supersaturation of the solutes. The kinetics of the growth and formation of solute clusters, or G–P zones, is largely controlled by the diffusivity of solute atoms, which, in turn, is directly related to the vacancy concentration. An investigation of solute atom segregation close to grain boundaries has been studied by Doig and Edington [14], using Al–Zn–Mg alloy. In general, the width of the precipitate-free zone increases with ageing temperature and decreases with increased solution treatment temperature [15]. It has also been observed that the precipitate-free zone width at a sub-boundary is always narrower than the zone width at a high angle boundary.

In this work, the widths of the precipitate-free zones at the subgrain boundaries were found to be less than 0.05 μm for samples aged at 110° C; in most cases, at this ageing temperature, the precipitate-free zone is not clearly observable. The phenomena can be explained in terms of the high nucleation rate of the G–P zones within the matrix and the competitive growth rate of precipitates on subgrain boundaries. Such precipitate-free zones on the subgrain boundaries have not been observed both in samples aged at 142° C and at 165° C. For the samples with short ageing times, the η-phase precipitation is still inhibited within the subgrains, and there is therefore no possibility of a precipitate-free zone. For longer ageing times, the solute atoms and vacancies approach a more uniform distribution inside the subgrains, the η-phase appears to be more abundant and distributed more uniformly and, again, no precipitation-free zone is seen.

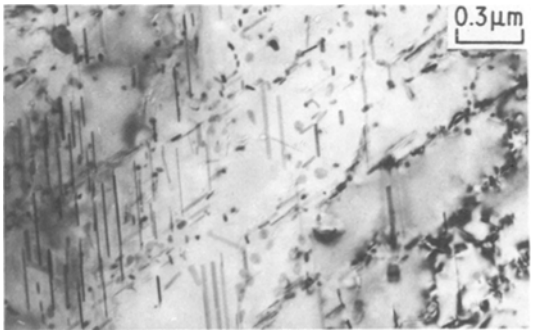

Figure 10 TEM view of specimen aged at 165° C for 5 h.

According to the microstructure studies made of the samples aged at 142° C and 165° C, the density of η-phase precipitates increases with ageing time in grains which contain no subgrain and in subgrains far away from the grain boundaries, as shown in Figs 7 and 8. This can be explained in terms of a vacancy depletion mechanism and the direct nucleation of the η-phase. In the absence of second vacancy sinks, i.e. subgrain boundaries, the vacancy concentration is largely retained inside the grain. Inside the subgrains which are far from a grain boundary, the depletion of the vacancy concentration due to the subgrain boundaries is much less effective and the vacancy concentration is also largely retained; besides, the subgrain boundaries act as much less effective vacancy sinks and this can explain why the subgrain boundary precipitation-free zone in the samples aged at 110° C is so narrow.

The variation of yield strength, ultimate tensile strength and elongation of the samples aged at 110° C, 142° C and 165° C for various ageing times are shown in Figs 12, 13 and 14, respectively.

Both the yield strength and the ultimate tensile strength of the alloy aged at 110° C increase as the ageing time increases. The increase

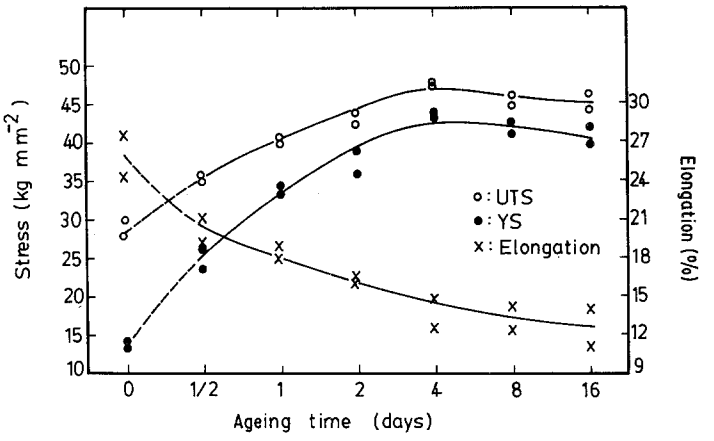

Figure 12 Stress and elongation plotted against ageing time for specimens aged at 110° C.

in strength is attributed to the presence of small, fine G–P zones and η'-phase plates. Because of the presence of η-phase regions and because the spacing of the η'-plates increases if the ageing time is greater than 96 hours, the strengths start to decrease.

The variation of the strengths of the alloys aged at 142° C and 165° C are similar; the variations of the appearances of the microstructures with ageing time are also similar for both series. The increase in yield strength is due to the dispersion hardening of η-phase precipitates in the matrix and the subgrain strengthening resulting from the η-phase precipitates lying on the subgrain boundaries. The elongation of the specimens at all three ageing temperatures decreased continuously with ageing time; this may be a result of the growth of the equilibrium phase on the grain boundaries and subgrain boundaries.

The variation of yield strength and ultimate tensile strength with strain rate was studied in specimens before ageing and in specimens aged at 165° C for 1 h for alloys with and without subgrains. The results are shown in Figs 15 and 16. Both the yield strength and the ultimate tensile strength decreased as the strain rate was increased. This phenomena, known as the inverse strain rate sensitivity, is a characteristic phenomenon of dynamic strain ageing or serrate yielding; the phenomena is also commonly called the Portevin–LeChatelier effect and is due to the pinning of dislocations by the solute atmosphere. The serrated phenomenon decreased with increased ageing time as the solute atom density decreased. Usually serrated yielding is observed when the strain rate is lower than $4.2 \times 10^{-3}\,\text{sec}^{-1}$.

4. Conclusions

(1) The ageing sequences for the three ageing temperatures have been determined as follows:

(i) SSS → G–P zones → η' → η ($MgZn_2$) (110° C)

(ii) SSS → η ($MgZn_2$) (142° C and 165° C).

(2) The widths of precipitate-free zones at the subgrain boundaries of specimens aged at 110° C were very narrow (less than 0.05 μm) and were usually unobservable. This has been attributed to the low sinking effect of vacancies with the low-angle subgrain boundaries which leads to the

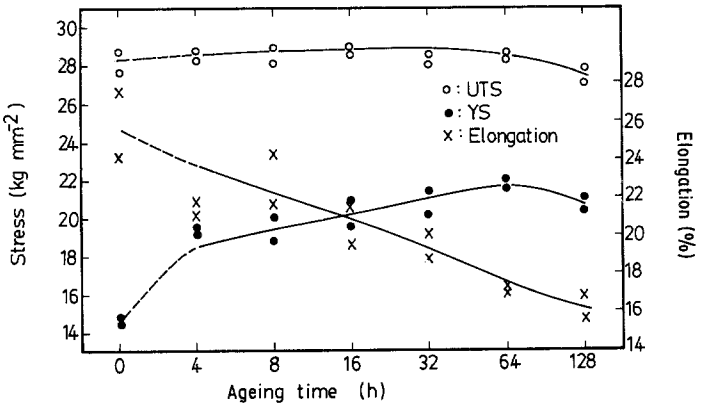

Figure 13 Stress and elongation plotted against ageing time for specimens aged at 142° C.

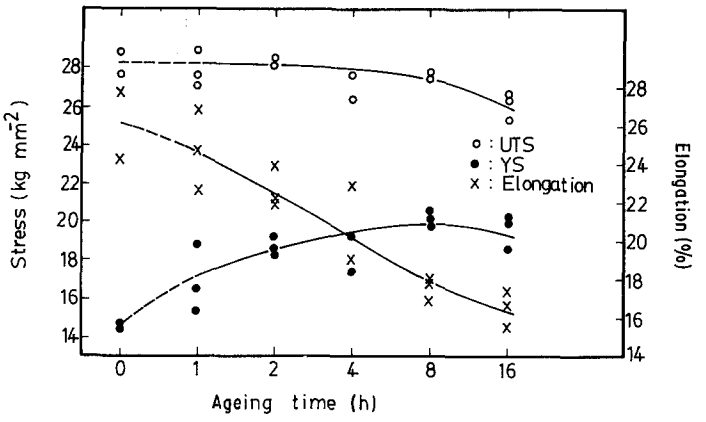

Figure 14 Stress and elongation plotted against ageing time for specimens aged at 165° C.

competitive growth rates of the precipitates on subgrain boundaries and the G–P zones within the matrix.

(3) The precipitate-free zone along the subgrain boundaries of specimens aged at 142° C and 165° C was always too narrow to be detected. This was due to the depletion of the precipitations inside the subgrain. In addition, most η-precipitates were observed first at the region close to the subboundaries, and they approach the area inside the subgrains during the ageing process.

(4) In specimens aged at 142° C and 165° C the nucleation of the η-phase was still inhibited in some subgrains near the regular grain boundary, even after very long ageing times; this was due to the depletion of the vacancies of both subgrain boundaries and grain boundaries.

(5) The precipitates which appear at the subgrain boundaries and grain boundaries led to the small elongation of specimens studied in this experiment.

(6) Serrated yielding was observed in the specimens aged at 165° C; this phenomenon decreased as the ageing time was increased and was observed for strain rates lower than 4.2×10^{-3} sec^{-1} at room temperature.

References

1. L. MONDOLFO, N. A. GJOSTEIN, and D. W. LEVINSON, *Trans. AIME* **206** (1956) 1378.
2. C. E. LYMAN and J. B. VANDER SANDE, *Met. Trans.* **7A** (1976) 1211.
3. J. GJØNNES and C. J. SIMENSEN, *Acta. Met.* **18** (1970) 881.
4. A. J. DEARDO, Jr and C. J. SIMENSEN, *Met. Trans.* **4** (1973) 2413.
5. P. A. THACKERY, *J. Inst. Metals* **96** (1968) 228.
6. J. WALDMAN, H. SULINSKI and H. MARKUS, *Met. Trans.* **5** (1974) 573.
7. N. RYUM, *Acta. Met.* **17** (1969) 831.
8. H. A. HOLL, *Metal Sci. J.* **1** (1967) 111.
9. V. V. ZAKHAROV, V. I. YELAGIN and L. I. LEVIN, *Fiz. Metal. Metalloved* **40** (1975) 102.
10. C. M. WAN, M. T. JAHN, T. Y. CHEN and L. CHANG, *J. Mater. Sci.* **13** (1978) 2059.
11. J. NUTTING, *Met. Trans.* **2** (1971) 45.
12. I. J. POLMEAR, *J. Inst. Metals* **87** (1958–59) 24.
13. P. N. T. UNWIN, G. W. LORIMER and R. B. NICHOLSON, *Acta. Met.* **17** (1969) 1363.
14. P. DOIG and J. W. EDINGTON, *Met. Trans.* **6A** (1975) 943.
15. J. D. EMBURY and R. B. NICHOLSON, *Acta Met.* **13** (1965) 403.

Received 29 May and accepted 6 November 1980.